Efficient *In Silico* Assay of Inhibitors of Hepatitis C Virus RNA-Dependent RNA Polymerase by Structure-Based Virtual Screening and *In Vitro* Evaluation

Ying-Ting Lin,[1,2,]* Kuo-Jung Huang,[1] Chin-kai Tseng,[1]
Kuan-Jen Chen,[1] Hui-Min Wang,[3] and Jin-Ching Lee [1,4,]*

[1]Department of Biotechnology, College of Life Sciences,
Kaohsiung Medical University, Kaohsiung, Taiwan.
[2]Center of Excellence for Environmental Medicine,
Kaohsiung Medical University, Kaohsiung, Taiwan.
[3]Department of Fragrance and Cosmetic Science,
Kaohsiung Medical University, Kaohsiung, Taiwan.
[4]Graduate Institute of Natural Products, College
of Pharmacy, Kaohsiung Medical University,
Kaohsiung, Taiwan.

ABSTRACT

To identify a new protective or therapeutic intervention for hepatitis C virus (HCV) infection, we performed efficient structure-based virtual screening to identify novel inhibitory agents for HCV. To this end, we selected NS5B, an RNA-dependent RNA polymerase (RdRp), as the target for the treatment of HCV infection. To decipher the dockable nature of various RdRp X-ray crystals, we docked the crystal ligand (inhibitor) to the crystal receptor (enzyme). The accuracy of regeneration of the crystal pose indicates the amenability of the RdRp binding pocket for structure-based virtual screening. We also utilized a consensus scoring scheme to reduce false positives, thereby ensuring efficient virtual screening. In this study, each molecule that ranked in the top 1% among all screening molecules gained 1 consensus point in a scoring function. Thus, after virtual screening of 57,177 chemicals from the Maybridge Screening collection, 14 molecules gained 8 points across 11 scoring functions. One of them, an isoxazole, showed significant dose-dependent inhibition of HCV RdRp activity and replication. In this study, we have developed a structure-based virtual screening method using HCV RdRp for efficient identification of novel inhibitors.

INTRODUCTION

Nearly 175 million people worldwide, ∼3% of the human population,[1] are carriers of the hepatitis C virus (HCV), and strikingly, 3–4 million individuals are newly infected each year. More than 70% of infected individuals develop chronic syndromes after HCV infection. A significant portion of liver-related morbidity and mortality, liver cirrhosis, and hepatocellular carcinomas[2,3] occur as a result of chronic HCV infection. End stage of severe liver disease can necessitate liver transplantation or lead to death.[4] No vaccine is available for HCV prevention and the current standard of care in treating chronic HCV infection consists of pegylated interferon alpha (IFN-α) combined with the nucleotide analog ribavirin (RBV), administered for 12–72 weeks.[5,6] Unfortunately, only about 50% of the individuals infected with HCV genotypes 1 and 4 obtained a sustained virological response to the current treatments, whereas 80% of patients infected with HCV genotype 2 or 3 obtained a sustained virological response.[7] Moreover, IFN-α and RBV treatment is associated with adverse effects, such as anemia and depression,[6] which often lead to discontinuation of the therapy.[8] Thus, the genotype-dependent responses and side effects necessitate the need for a novel, safer, and more effective agent against HCV infection.

The HCV is a positive-sense single-strand RNA virus and a member of the Hepacivirus genus within the family Flavivirida.[9] The 9.6-kb genome of HCV translates to a single viral polyprotein composed of about 3,000 amino acids including four structural proteins (C, E1, E2, and p7) and six nonstructural proteins (NS2, NS3, NS4A, NS4B, NS5A, and NS5B).[10,11] Among the nonstructural proteins, NS5B, an RNA-dependent RNA polymerase (RdRp),[12] is essential for viral RNA replication and has been considered as an attractive target for the chemotherapeutic inhibition of HCV infection.[13,14] The structure of RdRp has been extensively characterized by using X-ray crystallography.[15–31] This structural information provides a strong base for the development of an efficient structure-based virtual screening method for new anti-HCV agents.

AU1

In this research, we attempted to develop an efficient, structure-based virtual screening procedure for identifying novel anti-HCV agents. Most of the resolutions of the X-ray protein crystals in the Protein Data Bank (PDB) are lower than 2 Å, and this error could interfere with the high hit rate of structure-based virtual screening. If a 2-Å error occurs at the binding site, time and money would be wasted. To overcome this intrinsic flaw of crystallography, we docked the crystal inhibitor back into the crystal enzyme to identify the suitability of crystal proteins for virtual screening. At the same time, the optimal parameters of docking were optimized. We also used the consensus scoring scheme to reduce the false positives. To test the candidates for virtual screening, we used a replicon system[32] for HCV replication and an RdRp activity assay[33] for testing the inhibitory activity of RdRp's function. Results showed that 14 potential drug candidates, downsized from a total of 57,177 chemicals, earned the highest consensus scoring points, 8, among 11 scoring functions. The screening molecules were then purchased from the Maybridge Screening Collection (Maybridge Chemical Library, Thermo Fisher Scientific).[34] One of them appeared to inhibit HCV virus replication. Further dose-dependent tests of the RdRp activity assay showed inhibitory activity specific to HCV RdRp.

EXPERIMENTAL

Best Crystal Structure and Binding Pocket Selection

For enhancing the hit rate of the virtual screening for HCV NS5B, we examined the 26 three-dimensional complex crystals of HCV RdRp obtained from the PDB. According to the position of inhibitor binding sites, the complex crystals were divided to central or "palm" domain[35,36] (PDB code: 1YVF,[23] 2AWZ,[25] 2AX0,[25] 2AX1,[25] 2FVC,[26] 2GC8,[18] 2GIQ,[20] 2IJN,[28] 2QE2,[37] 2QE5[37]) and "thumb" domain[35,36] (PDB code: 1NHU,[27] 1NHV,[27] 1OS5,[22] 2BRK,[16] 2BRL,[16] 2DXS,[19] 2GIR,[20] 2HAI,[21] 2HWH,[38] 2HWI,[38] 2I1R,[30] 2O5D,[29] 3CIZ,[15] 3CJ0,[15] 3CJ2,[15] 3CJ3,[15] 3CJ4,[15] 3CJ5,[15] 3BSA,[31] 3BSC,[31] and 3BR9[31]). In each crystal complex, the crystal inhibitor was removed, leaving the binding site empty. Each complex inhibitor structure was randomized and then subjected to the molecular mechanics optimization, MMFF94[39,40] in ChemBioOffice 2008 package (CambridgeSoft Corporation), and docking it back to the original binding sites. We used LigandFit in Accelrys Discovery Studio 2.0 package (Accelrys) as our virtual screening and docking tools. The spatial root-mean-square deviation (RMSD) was calculated between the crystal pose and the after-docking pose. The lowest RMSD of 0.203 Å for the crystal inhibitor of 3CJ2 indicates both the correctness of the quality of the 3CJ2 crystallization and our HCV RDRP virtual screening procedure.

Docking and Consensus Scoring

LigandFit (Accelrys Software) is a docking strategy designed for high-throughput screening and for accurately docking ligands into protein binding sites. Some significant designs are as follows: a cavity detection algorithm is adopted for candidate active site regions. A Monte Carlo shape-based method is used for matching the ligand conformation into the active site shape. A grid-based method is to optimize ligand binding conformation for lowering the protein–ligand interaction energies. To reduce errors from grid interpolation, a nonlinear interpolation scheme, that is, a soft van der Waals potential and a soft electrostatic potential, was designed by developers.[41] In this study, the optimal docking cavity is expanding the occupied space of crystal 3CJ2 ligand by setting the ligand hydrogen radius to 2.0 Å and the heavy ligand atom to 2.5 Å. Crystal protein residues around binding sites are not allowed to move. Note that various scoring functions exist and differ in the descriptions of protein–ligand interactions. The interactions include a variety of sophisticated forms of noncovalent interactions, such as polar interactions, nonpolar interactions, solvent effect, and entropy effect. Different scoring functions perform differently in different types of protein complexes. No single scoring function can handle all equally excellent. In this study, the performances of 11 scoring functions were considered, which are LigScore1,[41] LigScore2,[41] DockScore,[41] PMF,[42] PMF04,[43] Ludi1,[44,45] Ludi2,[44,45] Ludi3,[46] PLP1,[47,48] PLP2,[47,48] and Jain.[49] If the compound's score of a particular scoring function rank within top 1%, the compound gains 1 point for consensus scoring. Maybridge compounds after virtual screening gaining 8 points among 11 scoring functions were purchased for further anti-HCV activity tests.

In Vitro HCV RdRp Activity Assay

Renilla luciferase reporter activity developed by us[32] represents the HCV RdRp activity. BHK-NS5B-FRLuc reporter cells were seeded in a 24-well plate at a density of 4×10^3 cells per well and treated with the compound in various concentrations. After incubation at 37°C for 4 days, cells lysates were harvested to measure the reporter gene expression inside the cell by using the Dual-GloTM Luciferase Assay System (Promega Corporation) following the manufacturer's instructions. The relative activity of NS5B polymerase was determined by normalizing the level of *Renilla* luciferase against the level of Firefly luciferase.

In Vitro HCV Cellular Replication Assay

The activity of HCV cellular replication is represented by the levels of NS5B protein in the Huh7-harboring HCV subgenomic replicon cells, designed Ava5. The Ava5 cells were kindly provided by Dr. C. Rice (Rockefeller University, NY)[50,51] and were maintained in Dulbecco's modified Eagle's medium with 10% heat-inactivated fetal bovine serum, 5% antibiotic–antimycotic, 5% nonessential amino acids, and 1 mg/mL G418 and incubated at 37°C with a 5% CO_2 supplement. The Ava5 cells were seeded in a six-well plate at a density of 2×10^5 cells per well and treated with the compound at various concentrations. After incubation at 37°C for 4 days, total cellular RNA was extracted using Trizol reagent (Invitrogen). The levels of HCV subgenomic RNA were detected by RT-quantitative polymerase chain reaction (RT-qPCR) with primers corresponding to NS5B gene; forward primer 5′-GGA AAC CAA GCT GCC CAT CA-3′, and reverse primer 5′-CCT CCA CGG ATA GAA GTT TA-3′. The copy number of HCV RNAs in each sample was normalized to cellular glyceraldehyde 3-phosphate dehydrogenase (forward primer: 5′-GTC TTC ACC ACC ATG GAG AA-3′; reverse primer: 5′-ATG GCA TGG

ACT GTG GTC AT-3′) levels from three independent experiments with the ABI Step One Real-Time PCR-System (ABI Warrington). Briefly, real-time PCR was carried out in 10 μL reaction volume containing 200 ng cDNA, 5 μL Power SYBR Green PCR Master Mix, and 0.4 μM primer pair. The PCR was conducted under the following conditions: denaturation at 95°C for 10 min, 40 cycles of amplification at 95°C for 15 s, 60°C for 1 min, and finally, 95°C for 15 s, 60°C for 1 min, and 95°C for 15 s.

Cytotoxicity Assay

Cell viability was determined by the colorimetric 3-(4,5-dimethylthiazol-2-yl)-5-(3-carboxymethoxyphenyl)-2-(4-sulfophenyl)-2H-tetrazolium (MTS) assay as described previously.[32] The Ava5 and BHK-NS5B-FRLuc-1 cells were seeded in a 96-well plate at densities of 5×10^3 and 8×10^2 cells per well, respectively, and treated with the compound at various concentrations. The CellTiter 96® AQueous One Solution Cell Proliferation Assay (Promega) was used to determine the cell viability after 4 days of incubation. The absorbance was detected at 490 nm.

Statistical Analysis

GraphPad Prism (version 5.0; SmartDrawNet) was used for all statistical analyses and graphical illustrations. Data were presented as means ± standards deviation for at least three independent experiments. The statistical significance was analyzed by using Student's t-test. The significant difference was considered as $P < 0.05$ or $P < 0.01$.

RESULTS
Binding Pocket Selection

We attempted to conduct a highly accurate (high hit rate) structure-based virtual screening for HCV with limited number of chemicals. X-ray crystallography can resolve structure at the atomic level and provide comprehensive structural insights. However, the average resolution as mentioned above is still not good enough for efficient structure-based virtual screening of HCV. The average resolution of the available RdRp crystals in the PDB was calculated to be 2.16 Å. This resolution factor as aforementioned could decrease the efficiency and accuracy of virtual screening, and this could lead to extra cost and time or even result in failure. Thus, the quality of the "dockable nature" of the binding pockets from crystal complexes under equal screening methodologies must be examined. To check the amenability of the crystal complexes for docking, we adopted a re-docking procedure in which a structure-randomized crystal ligand was docked back into the original crystal binding pocket. The spatial overlap between the crystal's pose (the X-ray bound pose) and the after-docking pose of the crystal inhibitor was calculated by RMSD. The regain of ligand crystal pose is usually one of central criteria for the feasibility of docking method,[52] but here we attempted to emphasize the suitability of crystal binding sites. Under an "equal base" of docking procedure, by checking the RMSDs (*Table 1*), we assessed the quality of the binding site of each crystal complex. The results showed that the docking pose of the 3CJ2 inhibitor was almost

Table 1. A List of the Protein Data Bank IDs of Available RNA–Dependent RNA Polymerase Crystals and the Root–Mean–Square Deviations Between the Crystal Inhibitor Pose and the After–Docking Pose

| PDB ID	RMSD	Resolution (Å)	PDB ID	RMSD	Resolution (Å)
3CJ2	0.203	1.75	2QE2	1.403	2.9
2HAI	0.268	1.58	3CJ4	1.812	2.07
2BRK	0.28	2.3	1NHV	2.13	2.9
2GIQ	0.293	1.65	3BSC	2.321	2.3
2I1R	0.343	2.2	2IJN	2.367	2.2
1OS5	0.379	2.2	2AX0	2.432	2
3CJ5	0.387	1.92	3CJ0	2.468	1.9
2DXS	0.427	2.2	3BR9	2.649	2.65
2BRL	0.467	2.4	1NHU	2.783	2
1YVF	0.507	2.5	2GC8	2.873	2.2
2HWI	0.526	2	3CIZ	2.941	1.87
2GIR	0.694	1.9	3BSA	3.088	2.3
2O5D	0.766	2.2	2AX1	3.68	2.1
2QE5	0.826	2.6	2FVC	3.715	2
3CJ3	0.882	1.87	2AWZ	4.195	2.15
2HWH	1.29	2.3			

3CJ2, first listed, has the lowest RMSD and is considered to be amenable for structure-based docking.
PDB, Protein Data Bank; RMSD, root-mean-square deviation.

similar to the original crystal structure, with an RMSD of 0.203 Å. *Figure 1A* shows an almost ideal structural overlap of the crystal pose and the after-docking pose of the 3CJ2 inhibitor, labeled with the calculated RMSD. Thus, the binding site of 3CJ2 was used for the structure-based virtual screening of RdRp, as it did not require any modifications in surrounding crystal residues or other ligand-based information. *Figure 1B* shows the enlarged portion of the cocrystal inhibitor and its relative position on 3CJ2, located in between the thumb and palm domain. *Figure 1C* also represents the surrounding residues LEU418, MET423, THR427, SER476, ILE482, ALA486, LEU497, ARG498, ARG501, ARG505, ALA529, and TRP528. Further, while finding the lowest RMSD between the crystal pose and the docking pose, we simultaneously optimized the docking procedure.

Virtual Screening and Consensus Scoring

To lower the RMSD between the crystal pose and the docking pose, we extensively adjusted the docking parameters. At the same time,
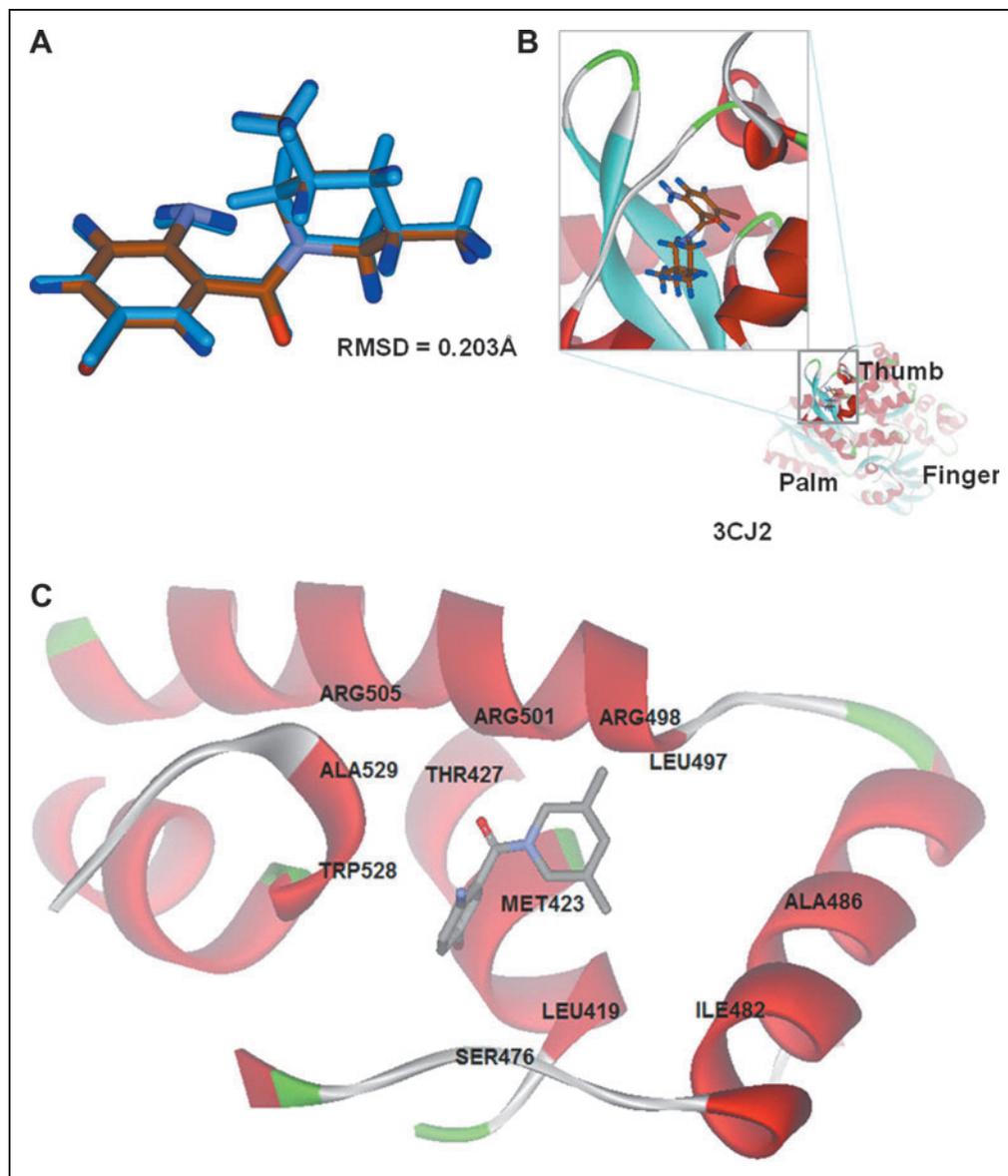
Fig. 1. **(A)** The spatial overlap between the crystal pose (dark blue color) and the after-docking pose (most brown color) of the 3CJ2 crystal inhibitor. The RMSD is 0.203 Å. **(B)** The X-ray binding mode of the crystal inhibitor in the HCV RdRp crystal complex (Protein Data Bank code: 3CJ2). The possible inhibitory mechanism could be an alteration in HCV RdRp breathing. **(C)** The surrounding residues of the binding pocket. RMSD, root-mean-square deviation; HCV, hepatitis C virus; RdRp, RNA-dependent RNA polymerase. Color images available online at www.liebertonline.com/adt.

library docking poses, by definition that compound gained 1 consensus point. The 14 molecules that gained more than 8 consensus points in the 11 scoring functions selected are listed in *Table 2*. These compounds were put into the HCV replication assay and the RdRp activity assay. The isoxazole CS01 (*Fig. 2A*) shows a significant inhibitory effect on HCV replication and RdRp activity. The IUPAC name of CS01 is 2-(2-nitro-4-(trifluoromethyl)phenoxy) phenyl 3-(2-chloro-6-fluorophenyl)-5-methylisoxazole-4-carboxylate. The inhibitor binding model (*Fig. 2B*) shows the docking pose of CS01 on HCV RdRp. Note that this binding site is thought to differ from the structural effect of nucleoside class (palm domain) and to possibly interfere with the breathing of RdRp, like the allosteric binding of 3CJ2 inhibitor (thumb).

Inhibition of RdRp Activity and HCV Replication

A cell-based RdRp reporter assay was recently described in our previous manuscript.[33] The RdRp activity was measured by a *Renilla* luciferase assay. To identify the RdRp inhibitors, 14 compounds from virtual screening with the concentration of 5 and 10 μM were put into the RdRp reporter screening, that is, testing for HCV replication. Of the chemicals used, CS01, shown in *Table 2*, exhibited an inhibitory effect on reporter activity compared with a well-characterized RdRp inhibitor 2′-C-methylcytidine (NM107),[53–56] which served as a positive control (*Fig. 3A*). Upon an

we obtained the best virtual screening procedure with optimal docking parameters. The docking details are described in the Experimental section. We used 57,177 molecules from the Maybridge Screening Collection[34] as the molecular screening library. To eliminate the false positives, we used a total of 11 scoring functions implemented in the LigandFit wizard to perform consensus scoring. After virtual docking, each molecule was given 11 scores. In this research, we adopted stringent criteria for limiting compounds. If the compound's score in a scoring function was within the top 1% of total

increase in the concentration of CS01, a significant reduction of reporter activity was observed, with the effective concentration of 50% inhibition (EC$_{50}$) value being $3.9 \pm 0.2\,\mu M$ (*Fig. 3B*). Notably, about 88% of the reporter activity was inhibited at a CS01 concentration of 15 μM, which showed no detectable cytotoxic effects by MTS analysis (data not shown). To further verify whether this compound can inhibit viral replication, HCV subgenomic replicon-harboring cells, Ava5, were incubated with increasing concentrations of CS01 for 4 days. RT-qPCR was then

VIRTUAL SCREENING OF COMPOUNDS AGAINST HCV RNA-DEPENDENT RNA POLYMERASE

| Table 2. Structures of 14 Molecules Gaining 8 Consensus Points in 11 Scoring Functions			
ID	**Structure**	**ID**	**Structure**
CS01		CS08	
CS02		CS09	
CS03		CS10	
CS04		CS11	
CS05		CS12	
CS06		CS13	
CS07		CS14	

The criterion is that if the compound's score belonging to a scoring function is within top 1% of total library docking poses, it gains 1 consensus point by definition.

performed to quantify intracellular HCV RNA. As shown in *Figure 3C*, CS01 reduced viral RNA levels significantly in a dose-dependent manner. The EC_{50} value, normalized for endogenous glyceraldehyde 3-phosphate dehydrogenase mRNA, was $6.1 \pm 0.3\,\mu M$. Similarly, MTS analysis failed to show cytotoxicity at levels up to $15\,\mu M$ of CS01 (data not shown). Taken together, our approach based on binding site selection, virtual screening, and consensus scoring successfully identified a novel compound that inhibits HCV RdRp activity and also blocks viral RNA replication.
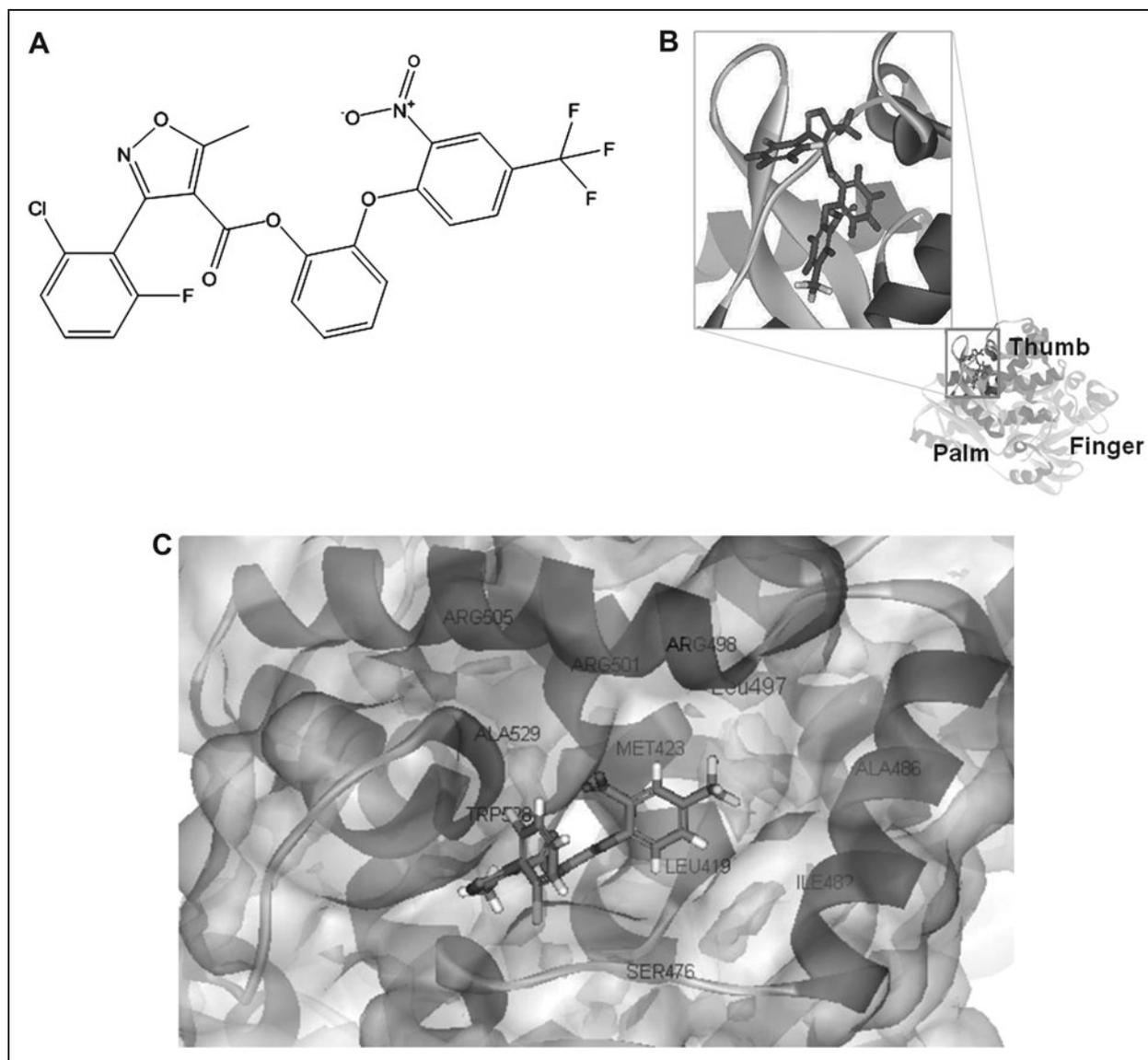
Fig. 2. (A) The chemical structure of the isoxazole CS01 (IUPAC name: 2-(2-nitro-4-(trifluoromethyl)phenoxy)phenyl 3-(2-chloro-6-fluorophenyl)-5-methylisoxazole-4-carboxylate). **(B)** The docking binding mode of CS01 in the HCV RdRp crystal complex (Protein Data Bank code: 3CJ2). The binding position of CS01 is in the thumb domain of HCV RdRp. The possible inhibitory mechanism could be an alteration in HCV RdRp breathing. **(C)** The surrounding residues of CS01 with the transparent polar or nonpolar surface. Blue color indicates negative charge, red color for positive, whereas light gray color means neutral.

DISCUSSION

In the present study, we identified a novel inhibitor of HCV RdRp through structure-based virtual screening with limited number of chemicals and *in vitro* RdRp assay. About 3–4 million individuals worldwide are expected to be infected with HCV each year. At present, no vaccine is available for HCV prevention, and the current therapy for chronic HCV infection combines IFN-α and the nucleotide analog RBV. Unfortunately, anemia and depression are common side effects of this treatment. The adverse side effects of current drugs necessitate an alternative therapy.[7] To successfully develop new anti-HCV drugs, it is essential to identify as many potential candidate drugs as possible. One of the promising target proteins of anti-HCV, NS5B, an RdRp[12] essential for the viral RNA replication, was chosen as the study target. In our experience, many structure-based virtual screenings fail or are not as efficient as expected. The factors responsible for this could be many: the strategy of virtual screening, the accuracy of scoring functions, or whether including ligand-based pharmacophore, and so on. Besides these, the resolution of the X-ray crystal itself could be a
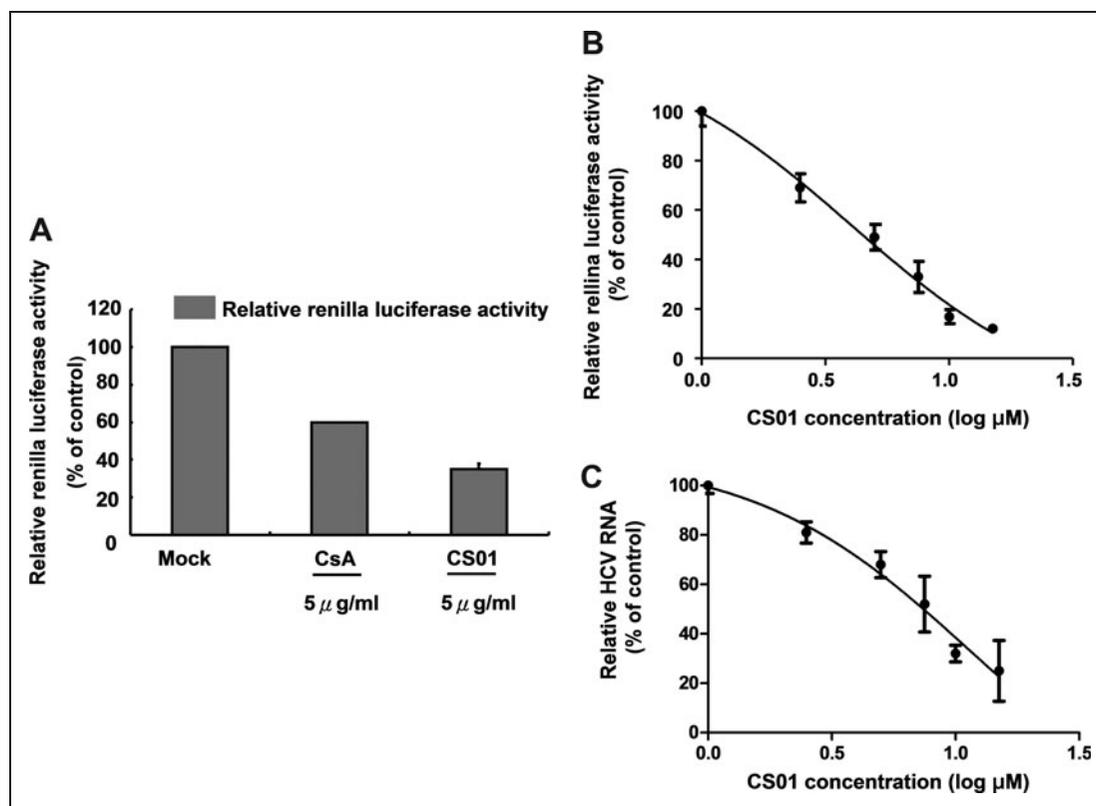
Fig. 3. The inhibitory effect of CS01 on HCV RdRp activity and replication. **(A)** Comparison of anti-RdRp activity between CS01 and a well-characterized RdRp inhibitor, NM107. BHK-NS5B-FRLuc-1 cells were treated with NM107 and CS01 at concentrations of 5 and 7.5 μM, respectively. After 4 days of incubation, total cell lysates were harvested to determine the luciferase activity. Mock indicates the treatment with 0.1% dimethyl sulfoxide. **(B)** Dose-dependent inhibition of CS01 on RdRp activity. BHK-NS5B-FRLuc-1 cells were treated with CS01 at various concentrations (1, 2.5, 5, 7.5, 10, and 15 μM) for 4 days. The effective concentration of 50% inhibition (EC_{50}) value of CS01 was 3.9 ± 0.2 μM for inhibition of luciferase activity. **(C)** Dose-dependent inhibition of CS01 on viral replication. Ava5 cells were treated with CS01 at various concentrations (1, 2.5, 5, 7.5, 10, and 15 μM) for 4 days. Relative amounts of HCV RNA were determined using RT-quantitative polymerase chain reaction analysis. The EC_{50} value of CS01 was 6.1 ± 0.3 μM. Each experiment was performed in triplicate, and the error bars reflect the standard deviations. The nonlinear regression graphs were used and the EC_{50} value was calculated using the GraphPad Prism5.0 program (version 5.0; SmartDrawNet).

crucial factor, as we know that a 2-Å deviation can lead to failure of structure-based virtual screening. Thus, for all available RdRp crystal complexes, it is essential to check whether the protein crystal is amenable for docking and virtual screening. One straight-forward way to do this is to adopt RMSD to examine the regenerated pose after a run of docking and to measure the spatial differences between the docking pose and the crystal pose. Under optimal docking settings, the 3CJ2 crystal inhibitor had the lowest RMSD (0.203 Å), which was far below the average RMSD of the available RdRp crystal inhibitors (2.16 Å). It must be noted that the resolution of the 3CJ2 X-ray crystal (1.75 Å) is higher than the average value (2.18 Å). In *Table 1*, the docking results show that better the X-ray resolution, higher will be the chances of regaining the crystal pose. The binding pockets around the palm part generally showed RMSDs above 3 Å, which are unsuitable for efficient structure-based virtual screening. The docking settings were simultaneously optimized when searching the lowest RMSD, like sampling of ligand conformation, grid energy, grid extension, interactions of rigid

body minimization, and so on. In addition to the resolution issue of X-ray crystals, the hydrogen atoms on crystal waters were totally missing because of the intrinsic characteristic of crystallography. This means that if we added hydrogen atoms to crystal oxygen, it would cause additional uncertainty, effecting the real orientation of hydrogen and impeding efficient docking. Thus, for the time being, we discounted and removed all crystal water oxygen atoms for virtual screening. Of 57,177 chemicals from the Maybridge Screening Collection, 14 chemicals gained 8 points among 11 scoring functions. One of them, analyzed under the newly developed RdRp activity assay, showed inhibitory activity similar to that of the well-characterized RdRp inhibitor, NM107. The hit rate was thus up to 7.1% when compared with a previous study[32] in which the hit rate was 2.3%. The two screening methods were only slightly different in the ways of handling consensus scoring, whereas the docking procedure was the same. On reviewing the literature, we found that virtual screening of drugs for HCV RdRp is limited, and the hit rate is generally below 1%. In the

present study, however, the hit rate as we expected would be much higher if we used cell-free assay. The reason for this is that the cell-free RdRp assay could eliminate the effects of drug metabolism, transportation, and toxicity. Thus, an in-house *in vitro* cell-free assay for anti-HCV RdRp activity is currently under development. In future, we plan to further refine the structure-based virtual screening procedure, both to improve the accuracy of the scoring function and to consider the effects of cell toxicity and drug transportation. Currently, virtual screening methods are being considered as promising approaches to accelerate drug discovery.[57–59] In the present study, we successfully identified a potent inhibitor of HCV NS5B by using a structure-based virtual screening of the Maybridge Screening Collection and the *in vitro* cell-based reporter assay. If more diverse potential drug candidates can be identified, then greater is the possibility of developing new therapies for inhibiting HCV. From the extensive interplay between *in silico* virtual screening and *in vitro* evaluation shown here, a more diverse structural core of potential inhibitors may be discovered. The new core can be further modified to improve its anti-HCV activity. In future, we hope that more potential drug candidates will be available, from which the most effective therapy for HCV, with minimum or no side effects, can be developed.

ACKNOWLEDGMENTS

DISCLOSURE STATEMENT

No competing financial interests exist.

REFERENCES

1. Koziel MJ, Peters MG: Viral hepatitis in HIV infection. *N Engl J Med* 2007;356:1445–1454.
2. McHutchison JG, Patel K: Future therapy of hepatitis C. *Hepatology* 2002;36(5 Suppl 1):S245–S252.
3. Williams R: Global challenges in liver disease. *Hepatology* 2006;44:521–526.
4. Sharma P, Lok A: Viral hepatitis and liver transplantation. *Semin Liver Dis* 2006;26:285–297.
5. NIH Consensus Statement on Magagement of Hepatitis C: 2002. *NIH Consens State Sci Statements* 2002;19:1–46.
6. Fried MW, Hadziyannis SJ: Treatment of chronic hepatitis C infection with peginterferons plus ribavirin. *Semin Liver Dis* 2004;24:47–54.
7. Soriano V, Peters MG, Zeuzem S: New therapies for hepatitis C virus infection. *Clin Infect Dis* 2009;48:313–320.
8. Schaefer M, Mauss S: Hepatitis C treatment in patients with drug addiction: clinical management of interferon-alpha-associated psychiatric side effects. *Curr Drug Abuse Rev* 2008;1:177–187.
9. Lindenbach BD, Rice CM: Unravelling hepatitis C virus replication from genome to function. *Nature* 2005;436:933–938.
10. Major ME, Feinstone SM: The molecular virology of hepatitis C. *Hepatology* 1997;25:1527–1538.
11. Penin F, Dubuisson J, Rey FA, Moradpour D, Pawlotsky JM: Structural biology of hepatitis C virus. *Hepatology* 2004;39:5–19.
12. Behrens SE, Tomei L, De Francesco R: Identification and properties of the RNA-dependent RNA polymerase of hepatitis C virus. *Embo J* 1996;15:12–22.
13. De Francesco R, Migliaccio G: Challenges and successes in developing new therapies for hepatitis C. *Nature* 2005;436:953–960.
14. Kwong A, McNair L, Jacobson I, George S: Recent progress in the development of selected hepatitis C virus NS3 4A protease and NS5B polymerase inhibitors. *Current Opin Pharmacol* 2008;8:522–531.
15. Antonysamy SS, Aubol B, Blaney J, *et al.*: Fragment-based discovery of hepatitis C virus NS5b RNA polymerase inhibitors. *Bioorg Med Chem Lett* 2008;18:2990–2995.
16. Di Marco S, Volpari C, Tomei L, *et al.*: Interdomain communication in hepatitis C virus polymerase abolished by small molecule inhibitors bound to a novel allosteric site. *J Biol Chem* 2005;280:29765–29770.
17. Gopalsamy A, Aplasca A, Ciszewski G, *et al.*: Design and synthesis of 3,4-dihydro-1H-[1]-benzothieno [2, 3-c] pyran and 3, 4-dihydro-1H-pyrano [3,4-b] benzofuran derivatives as non-nucleoside inhibitors of HCV NS5B RNA dependent RNA polymerase. *Bioorg Med Chem Lett* 2006;16:457–460.
18. Gopalsamy A, Chopra R, Lim K, *et al.*: Discovery of proline sulfonamides as potent and selective hepatitis C virus NS5b polymerase inhibitors. Evidence for a new NS5b polymerase binding site. *J Med Chem* 2006;49:3052–3055.
19. Ikegashira K, Oka T, Hirashima S, *et al.*: Discovery of conformationally constrained tetracyclic compounds as potent hepatitis C virus NS5B RNA polymerase inhibitors. *J Med Chem* 2006;49:6950–6953.
20. Le Pogam S, Kang H, Harris SF, *et al.*: Selection and characterization of replicon variants dually resistant to thumb- and palm-binding nonnucleoside polymerase inhibitors of the hepatitis C virus. *J Virol* 2006;80:6146–6154.
21. Li H, Tatlock J, Linton A, *et al.*: Identification and structure-based optimization of novel dihydropyrones as potent HCV RNA polymerase inhibitors. *Bioorg Med Chem Lett* 2006;16:4834–4838.
22. Love RA, Parge HE, Yu X, *et al.*: Crystallographic identification of a noncompetitive inhibitor binding site on the hepatitis C virus NS5B RNA polymerase enzyme. *J Virol* 2003;77:7575–7581.
23. Pfefferkorn JA, Greene ML, Nugent RA, *et al.*: Inhibitors of HCV NS5B polymerase. Part 1: evaluation of the southern region of (2Z)-2-(benzoylamino)-3-(5-phenyl-2-furyl) acrylic acid. *Bioorg Med Chem Lett* 2005;15:2481–2486.
24. Pfefferkorn JA, Nugent R, Gross RJ, *et al.*: Inhibitors of HCV NS5B polymerase. Part 2: evaluation of the northern region of (2Z)-2-benzoylamino-3-(4-phenoxy-phenyl)-acrylic acid. *Bioorg Med Chem Lett* 2005;15:2812–2818.
25. Powers JP, Piper DE, Li Y, *et al.*: SAR and mode of action of novel non-nucleoside inhibitors of hepatitis C NS5b RNA polymerase. *J Med Chem* 2006;49:1034–1046.
26. Tedesco R, Shaw AN, Bambal R, *et al.*: 3-(1,1-Dioxo-2H-(1,2,4)-benzothiadiazin-3-yl)-4-hydroxy-2(1 H)-quinolinones, Potent Inhibitors of Hepatitis C Virus RNA-Dependent RNA Polymerase. *J Med Chem* 2006;49:971–983.
27. Wang M, Ng KKS, Cherney MM, *et al.*: Non-nucleoside analogue inhibitors bind to an allosteric site on HCV NS5B polymerase. Crystal structures and mechanism of inhibition. *J Biol Chem* 2003;278:9489–9495.
28. Yan S, Appleby T, Gunic E, *et al.*: Isothiazoles as active-site inhibitors of HCV NS5B polymerase. *Bioorg Med Chem Lett* 2007;17:28–33.
29. Yan S, Appleby T, Larson G, *et al.*: Thiazolone-acylsulfonamides as novel HCV NS5B polymerase allosteric inhibitors: Convergence of structure-based drug design and X-ray crystallographic study. *Bioorg Med Chem Lett* 2007;17:1991–1995.
30. Yan S, Larson G, Wu JZ, *et al.*: Novel thiazolones as HCV NS5B polymerase allosteric inhibitors: further designs, SAR, and X-ray complex structure. *Bioorg Med Chem Lett* 2007;17:63–67.
31. Zhou Y, Webber SE, Murphy DE, Li L-S, Dragovich PS, Tran CV, Sun Z, Ruebsam F, Shah AM, Tsan M, Showalter RE, Patel R, Li B, Zhao Q, Han Q, Hermann T, Kissinger CR, LeBrun L, Sergeeva MV, Kirkovsky L: Novel HCV NS5B polymerase

inhibitors derived from 4-(1′,1′-dioxo-1′,4′-dihydro-1′lambda6-benzo[1′,2′,4′]thiadiazin-3′-yl)-5-hydroxy-2H-pyridazin-3-ones. Part 1: exploration of 7′-substitution of benzothiadiazine. *Bioorg Med Chem Lett* 2008;18:1413–1418.

32. Lee JC, Tseng CK, Chen KJ, Huang KJ, Lin CK, Lin YT: A cell-based reporter assay for inhibitor screening of hepatitis C virus RNA-dependent RNA polymerase. *Anal Biochem* 2010;9:9.

33. Lee J-C, Tseng C-k, Chen K-J, Huang K-J, Lin Y-T: Development of a cell-based reporter assay for inhibitor screening of hepatitis C virus RNA-dependant-RNA polymerase. *Anal Biochem* 2010;403:52–62.

34. McGregor MJ, Pallai PV: Clustering of large databases of compounds: using the MDL keys as structural descriptors. *J Chem Inf Comput Sci* 1997;37:443–448.

35. Ago H, Adachi T, Yoshida A, *et al.*: Crystal structure of the RNA-dependent RNA polymerase of hepatitis C virus. *Structure* 1999;7:1417–1426.

36. Weber PC, Lesburg CA, Cable MB, Ferrari E, Hong Z, Mannarino AF: Crystal structure of the RNA-dependent RNA polymerase from hepatitis C virus reveals a fully encircled active site. *Nat Struct Biol* 1999;6:937–943.

37. Nittoli T, Curran K, Insaf S, *et al.*: Identification of anthranilic acid derivatives as a novel class of allosteric inhibitors of hepatitis C NS5B polymerase. *J Med Chem* 2007;50:2108–2116.

38. Yan S, Appleby T, Larson G, *et al.*: Structure-based design of a novel thiazolone scaffold as HCV NS5B polymerase allosteric inhibitors. *Bioorg Med Chem Lett* 2006;16:5888–5891.

39. Halgren TA: MMFF VII. Characterization of MMFF94, MMFF94s, and other widely available force fields for conformational energies and for intermolecular-interaction energies and geometries. *J Comput Chem* 1999;20:730–748.

40. Halgren TA, Nachbar RB: Merck molecular force field. IV. conformational energies and geometries for MMFF94. *J Comput Chem* 1996;17:587–615.

41. Venkatachalam CM, Jiang X, Oldfield T, Waldman M: LigandFit: a novel method for the shape-directed rapid docking of ligands to protein active sites. *J Mol Graph Model* 2003;21:289–307.

42. Muegge I, Martin YC: A general and fast scoring function for protein-ligand interactions: a simplified potential approach. *J Med Chem* 1999;42:791–804.

43. Muegge I: PMF scoring revisited. *J Med Chem* 2006;49:5895–5902.

44. Böhm HJ: The development of a simple empirical scoring function to estimate the binding constant for a protein-ligand complex of known three-dimensional structure. *J Comput Aided Mol Des* 1994;8:243–256.

45. Böhm HJ: On the use of LUDI to search the fine chemicals directory for ligands of proteins of known three-dimensional structure. *J Comput Aided Mol Des* 1994;8:623–632.

46. Böhm HJ: Prediction of binding constants of protein ligands: a fast method for the prioritization of hits obtained from *de novo* design or 3D database search programs. *J Comput Aided Mol Des* 1998;12:309–323.

47. Gehlhaar DK, Verkhivker GM, Rejto PA, *et al.*: Molecular recognition of the inhibitor AG-1343 by HIV-1 protease: conformationally flexible docking by evolutionary programming. *Chem Biol* 1995;2:317–324.

48. Parrill A: *Rational Drug Design: Novel Methodology and Practical Applications*. American Chemical Society, Washington, DC, 1999.

49. Jain AN: Scoring noncovalent protein-ligand interactions: a continuous differentiable function tuned to compute binding affinities. *J Comput Aided Mol Des* 1996;10:427–440.

50. Goto K, Watashi K, Murata T, Hishiki T, Hijikata M, Shimotohno K: Evaluation of the anti-hepatitis C virus effects of cyclophilin inhibitors, cyclosporin A, and NIM811. *Biochem Biophys Res Commun* 2006;343:879–884.

51. Watashi K, Hijikata M, Hosaka M, Yamaji M, Shimotohno K: Cyclosporin A suppresses replication of hepatitis C virus genome in cultured hepatocytes. *Hepatology* 2003;38:1282–1288.

52. Irwin JJ, Shoichet BK, Mysinger MM, *et al.*: Automated docking screens: a feasibility study. *J Med Chem* 2009;52:5712–5720.

53. Murakami E, Niu C, Bao H, *et al.*: The mechanism of action of beta-D-2′-deoxy-2′-fluoro-2′-C-methylcytidine involves a second metabolic pathway leading to beta-D-2′-deoxy-2′-fluoro-2′-C-methyluridine 5′-triphosphate, a potent inhibitor of the hepatitis C virus RNA-dependent RNA polymerase. *Antimicrob Agents Chemother* 2008;52:458–464.

54. Gardelli C, Attenni B, Donghi M, *et al.*: Phosphoramidate prodrugs of 2′-C-methylcytidine for therapy of hepatitis C virus infection. *J Med Chem* 2009;52:5394–5407.

55. Pierra C, Amador A, Benzaria S, *et al.*: Synthesis and pharmacokinetics of valopicitabine (NM283), an efficient prodrug of the potent anti-HCV agent 2′-C-methylcytidine. *J Med Chem* 2006;49:6614–6620.

56. Coelmont L, Paeshuyse J, Windisch MP, De Clercq E, Bartenschlager R, Neyts J: Ribavirin antagonizes the *in vitro* anti-hepatitis C virus activity of 2′-C-methylcytidine, the active component of valopicitabine. *Antimicrob Agents Chemother* 2006;50:3444–3446.

57. Corbeil CR, Englebienne P, Yannopoulos CG, *et al.*: Docking ligands into flexible and solvated macromolecules. 2. Development and application of fitted 1.5 to the virtual screening of potential HCV polymerase inhibitors. *J Chem Inf Model* 2008;48:902–909.

58. Kim J, Kim KS, Kim DE, Chong Y: Identification of novel HCV RNA-dependent RNA polymerase inhibitors using pharmacophore-guided virtual screening. *Chem Biol Drug Des* 2008;72:585–591.

59. Ryu K, Kim ND, Choi SI, *et al.*: Identification of novel inhibitors of HCV RNA-dependent RNA polymerase by pharmacophore-based virtual screening and *in vitro* evaluation. *Bioorg Med Chem* 2009;17:2975–2982.

Address correspondence to:
Ying-Ting Lin
Department of Biotechnology
College of Life Sciences
Kaohsiung Medical University
100, Shih-Chuan 1st Road
San Ming District
Kaohsiung City 807
Taiwan
Republic of China

E-mail: ytlin@kmu.edu.tw

Jin-Ching Lee
Department of Biotechnology
College of Life Sciences
Kaohsiung Medical University
100, Shih-Chuan 1st Road
San Ming District
Kaohsiung City 807
Taiwan
Republic of China

E-mail: jclee@kmu.edu.tw

AU1   Please define RT in "RT-qPCR."

AU2   Please note that the "Experimental" section has been set before "Results" section. Hence, refs. 31–62 have been renumbered in sequential order. Also, please check the sentence "In this study, the optimal docking cavity is . . ." for clarity.

AU3   Refs. 31 and 32 are same. So Ref. 32 has been deleted.

AU4   Refs. 34 and 42 do not refer to published materials. Hence, they have been deleted from the Ref. list and inserted in the text.

AU5   Please mention the degrees of corresponding authors Ying-Ting Lin and Jin-Ching Lee.

AU6   In the legend of Fig. 3, the description "NM107 and CS01 at concentration of 5 and 7.5 μM" does not match with panel A. Please check.

AU7   Please expand RT in "RT-qPCR."